Alkaline hydrogen electrode and oxygen reduction reaction on PtxNi nanoalloys

C.A. Campos-Roldán, L. Calvillo, G. Granozzi, N. Alonso-Vante

Version of Record: https://www.sciencedirect.com/science/article/pii/S1572665719307179
Manuscript_261abab357d1ad0e223abbaec727567b

Alkaline Hydrogen Electrode and Oxygen Reduction Reaction on Pt_xNi Nanoalloys

C.A. Campos-Roldán[1,2], L. Calvillo[3], G. Granozzi[3], N. Alonso-Vante[1]*

[1]IC2MP, UMR-CNRS 7285, University of Poitiers, 4 rue Michel Brunet, 86022 Poitiers, France
[2]Instituto Politécnico Nacional-ESIQIE, Laboratorio de Electroquímica y Corrosión, UPALM, 07738, CDMX, México
[3]Department of Chemical Sciences, University of Padova, Via Marzolo 1, 35131, Padova, Italy

---

ABSTRACT

The electrochemical characterization of chemical carbonyl route generated Pt:Ni nano-alloys, in acid and alkaline media, is reported. Earlier XRD and Debye Function Analysis (DFA) studies [1] provided the structure of these nanoalloys. Herein, the HER/HOR electrocatalytic activity as well as ORR kinetics, in alkaline medium, was determined and correlated with the interatomic Pt-Pt distance. The HER/HOR and ORR exchange current densities describes a Volcano-like plot. For both systems, the maximum activity for both processes peaked with Pt_3Ni.

KEYWORDS
PtNi nanoalloys; Hydrogen electrode reaction; Oxygen reduction reaction; Alkaline medium

1. INTRODUCTION

The advances reached in the field of anion-exchange membrane (AEM) [2] are nowadays offering new important opportunities for a sustainable energy management based on fuel cells (FCs). Actually, the alkaline environment can provide the outlook to avoid the use of noble metals as electrocatalysts, so circumventing the critical raw materials issue. Innovative non-precious metal electrocatalysts, capable to activate the sluggish oxygen reduction reaction (ORR) and oxygen evolution reaction (OER) kinetics, are being developed, driving activity and stability similar or higher than Pt in alkaline medium [3-5]. On the other hand, the hydrogen evolution reaction (HER) and the hydrogen oxidation reaction (HOR) kinetics on precious-metal surfaces (Pt, Ru, Ir or Pd) is, certainly, sluggish in alkaline media,[6] representing a new challenge. In this regard, some efforts have been done to try to understand the determining mechanisms of the hydrogen electrode reaction (HER/HOR) on precious-metal catalytic centers, to extract useful information for tailoring non-precious based metal electrocatalysts. Following such a method, many researchers have pointed out a synergetic effect between Pt and Ni-based structures: metallic Ni [7-10], NiO [11] or $Ni(OH)_2$ [12-14] can improve the hydrogen electrode reaction kinetics, since the Ni-based domains can act as water dissociation sites, and reactive OH species adsorption sites. In addition, Ni can act as a Pt electronic-structure modifier, so modulating the Pt surface adsorption properties, as well as the reaction rate. Definitely, interesting approaches have been adapted to derive more insights to understand and, therefore, enhance the sluggish hydrogen electrode reaction in alkaline medium, taking Pt-based catalyst as a reference point. Such strategies range from the study of high-extended Pt surfaces decorated with $Ni(OH)_2$ domains in the nanoscale range, [12-14] or by tuning the Pt:Ni nanoalloy morphology, e.g., nanoparticles, nanowires [7-11]. Even though some inconsistency still exists regarding the kinetic descriptor [15], an enhanced HER/HOR performance is usually correlated with the weakening of the hydrogen binding energy and/or with the increased oxophilicity of the surface, which, in fact, is induced by the presence of Ni-based species. However, some structural properties could also enhance the electrocatalytic properties of Pt. Escudero et al. [16] provided evidence of the influence of Pt-Pt interatomic distance in Pt_5M, where M is lanthanide or alkaline earth elements towards the ORR in acid medium. They concluded that the lanthanide contraction can control the strain effects and tune the electrocatalytic performance of these materials. To the best of our knowledge, the above-mentioned effect has not been explored to enhance the hydrogen electrode reaction kinetics in alkaline medium.

In this work, we rationalize the effect of the Pt-Pt interatomic distances of carbon-supported Pt_xNi (x = 1, 2, 3 or 5) nanoalloys towards the hydrogen electrode reaction and the oxygen reduction reaction in alkaline medium. Surface electrochemistry was explored in acidic medium in order to contrast surface phenomena in the presence of OH species in alkaline medium.

2. EXPERIMENTAL

2.1. Carbon supported Pt_xNi synthesis

The carbon supported Pt_xNi (x = 1, 2, 3 or 5) were synthetized via the carbonyl chemical route [1]. These nanoalloys were subjected to a H_2-atmosphere annealing treatment, in the 200-500 °C temperature range, as earlier described [1].

2.2. Morphological and structural characterization

A detailed study of the morphology, particle size and structural properties of Pt_xNi/C electrocatalysts can be found in ref [1]. In the Tables 1 and 2, of reference [1], the most important properties of the studied Pt_xNi/C materials are summarized. The nanoalloy materials, with a mean particle size of 2.7 nm, were stable in time as confirmed by recent XRD measurements, after a long aging (stored in vials), performed specifically on Pt_2Ni and Pt_3Ni.

2.3. Inductively Coupled Plasma Optical Emission Spectroscopy measurements

10-15 mg of solid sample was dissolved into 50 mL of an acid mixture (2.5 mL of > 68% HNO_3, 2 mL of 34-37% HCl, 0.5 mL of 47-51% HF, 3 mL of H_3BO_3 and 42 mL of water. The final volume was 50 mL). The total mineralization was realized in a microwave oven (Anton-Paar Multiwave Pro) with 600 W for 40 min.

2.4. X-ray photoemission spectroscopy measurements

X-ray photoemission spectroscopy (XPS) measurements were performed at room temperature in a custom designed UHV system equipped with an Omicrom electron analyzer, working at a base pressure of 10^{-10} mbar. The Pt 4f, C 1s, O 1s and Ni 2p photoemission lines were acquired in normal emission using a non-monochromatized Mg K_α X-ray source (1253.6 eV). Single spectral regions were collected using 0.1 eV steps, 0.5 s collection time and 20 eV pass energy. For the deconvolution analysis, Voigt shaped peaks were used, imposing a FWHM in the 1–1.5 eV range, except for the metallic Pt component where an asymmetrical shape was used.

2.5. Electrochemical measurements

All measurements were carried out following the experimental protocol reported in ref. [17]. The catalytic ink was prepared by blending 5 mg of catalyst and 1 mL of stock solution (20 % v/v isopropanol, 0.4 % v/v ionomer and 79.6 % v/v deionized water). Nafion® 5% v/v was used as ionomer for measurements in acid electrolyte; whereas AS-4 Tukuyama® 5% v/v ionomer was used in alkaline electrolyte. The catalytic powder in the ink was dispersed in an ultrasonic bath for 30 min. Then, 3 µL of this suspension was dropped onto a glassy carbon electrode (3 mm dia.) and dried at room temperature by rotating the electrode at 700 rpm. The electrochemical measurements were carried out in a 0.1M KOH solution (pH ca. 13) using a potentiostat/galvanostat (Autolab PGSTAT 30). All experiments were performed in a single-compartment PTFE cell to avoid any contact between the electrolyte and glass surfaces [18]. The PTFE cell was provided with

a glass jacket connected to a calibrated thermostat at 25 °C. A Pt mesh and a mercury oxide electrode (E= -0.92 V vs. RHE) were, respectively, used as counter and reference electrodes. All potentials in this work are quoted against the reversible hydrogen electrode (RHE). Cyclic voltammetry (CV) was carried out from 0.05 to 1.0 V, at 50 mV s^{-1}, with N_2-saturated electrolyte. ORR and HER/HOR polarization curves were recorded, respectively, in oxygen-, and hydrogen-saturated electrolyte, maintaining a constant pressure of 100 kPa [19], at 5 mV s^{-1}, at different rotation rates (400, 900, 1600 and 2500 rpm). Finally, the ohmic drop was determined by electrochemical impedance spectroscopy, applying a perturbation of 5 mV rms (1 MHz to 0.1 Hz). The cell resistance was estimated from the linearly extrapolated intercept with the real x-axis in the Nyquist diagram. The resistance was ca. 40-45 Ω.

3. RESULTS AND DISCUSSION

3.1. Chemical-, and electronic-environment

In order to identify the predominant oxidation state of Pt and evaluate if the addition of Ni has any effect on the Pt electronic environment, the samples were investigated by XPS. The Pt 4f photoemission lines, Figure 1, were separated into three different chemically shifted components, after Shirley background removal. The results derived from the deconvolution of the Pt 4f photoemission lines are summarized in Table 1.

Table 1. Analysis of the Pt 4f photoemission line for the carbon supported Pt-Ni materials. For each single chemical component, the BE (eV) and amount (at. %) values are given.

Material	Pt^0	Pt^{2+}	Pt^{4+}	Ni	NiO
Pt/C JM	71.1 eV 69.0 %	72.6 eV 17.0 %	74.2 eV 14.0	NA	NA
PtNi/C	71.0 eV 77.7 %	72.7 eV 15.2 %	74.4 eV 7.1 %	31.2 %	68.8 %
Pt_2Ni/C	71.0 eV 82.1 %	72.7 eV 12.1 %	74.2 eV 5.8 %	25.9 %	74.1 %
Pt_3Ni/C	71.1 eV 69.0 %	72.8 eV 17.5 %	74.2 eV 13.5 %	21.0 %	79.0 %
Pt_5Ni/C	71.0 eV 83.2 %	72.7 eV 11.3 %	74.3 eV 5.5 %	15.6 %	84.4 %

The main component is centered at around 71.0 eV, indicating that Pt^0 is the predominant oxidation state in all the Pt catalysts. All the samples contain a variable amount of oxidized species as the components at 72.7 eV and 74.3 eV, assigned to Pt^{2+} and Pt^{4+} ions. The presence of oxidized species can be attributed to the oxidation of surface Pt atoms due to the contact with air. Our XPS data do not single out significative BE shifts along the series. We retain that this is an intrinsic limitation of the technique when applied to powder complex samples.

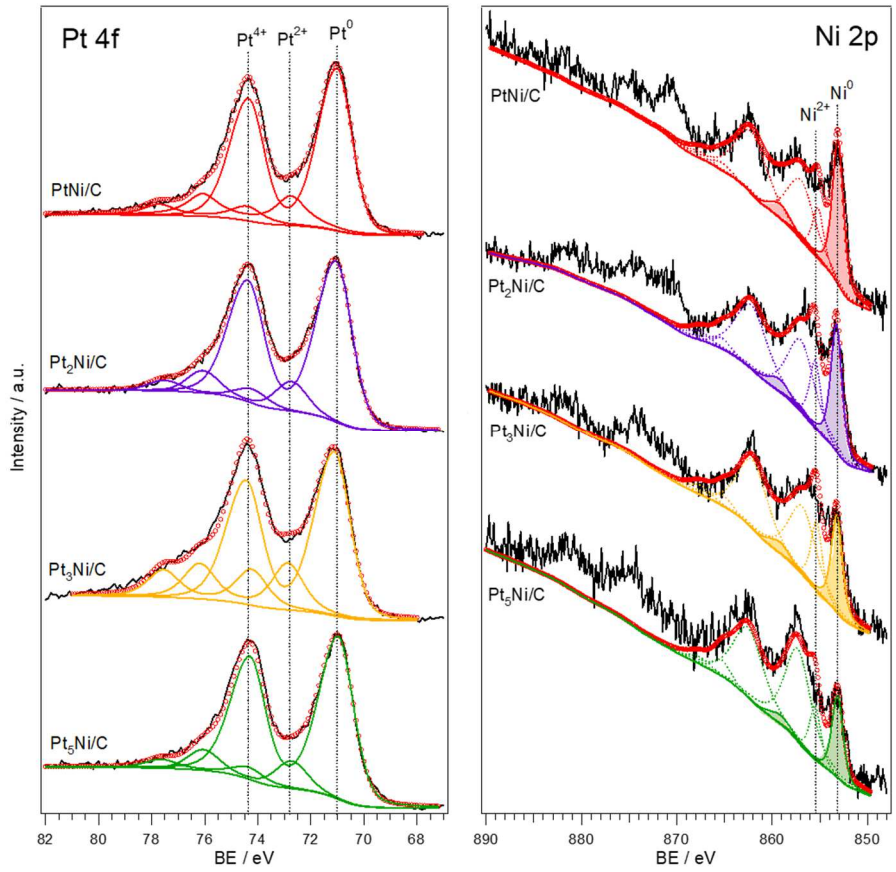

Figure 1. Pt 4f and Ni 2p photoemission lines for the carbon supported Pt_xNi/C materials, as well as the deconvolution of both regions into chemically shifted components.

Regarding the Ni 2p region, shown in Figure 1, the Ni $2p_{5/2}$ was deconvoluted into two main components at 853.2 eV and 855.3 eV, which could be associated to metal Ni and NiO, respectively. Both components show a complex multiplet splitting, shake-up and plasmon loss structure, that were taken into account for the deconvolution, as reported in ref [20]. As set out in Figure 1, the amount of metallic Ni increases with the amount of Ni in the sample, indicating concomitantly the Pt-Ni alloy formation. The amount of all the Ni components derived from the fit are reported in Table 2.

Table 2. Surface composition of the carbon supported Pt-Ni materials calculated from XPS analysis.

Material	Pt (at.%)	Ni (at.%)	C (at.%)	O (at.%)	Pt:Ni
PtNi/C	4.5	3.6	86.4	5.5	1.25:1
Pt_2Ni/C	6.9	7.9	73.7	11.5	0.87:1
Pt_3Ni/C	7.7	4.3	80.6	7.4	1.8:1
Pt_5Ni/C	6.1	4.3	74.6	15.0	1.4:1

The surface composition, Table 2, of the Pt-Ni samples was calculated from the area of the high-resolution spectra, taking into account the corresponding sensitivity factors. For all the samples, except for the 1:1 Pt:Ni, a higher amount of Ni is observed, indicating a surface segregation of this metal induced by the NiO formation in contact with air, in spite of the fact that the surface energy for Pt (2.35 J/m^2) is lower than that of Ni (2.45 J/m^2) [21]. The ICP analysis of all samples is consistent with the nominal stoichiometry

for all the analyzed samples. These results compared to those obtained by XPS, Table 3, clearly specify the difference in the composition of the nanoparticulated alloys.

Table 3. Pt/Ni surface composition comparison of Pt_xNi/C and Pt/C JM catalysts.

Catalysts	Pt-Pt distance (nm) [1]	(wt.%)Pt : (wt.%)Ni[1]	*wt.%Pt:wt.%Ni	*Pt:Ni (at. %)	*ICP-bulk Stoichiometry	‡XPS- Surface Stoichiometry
†Pt/C JM	0.2774	†100	†20 : 0	†100 : 0	†Pt	†Pt
[a]PtNi/C	0.2689	56 : 44	18.6 : 0.94±0.89	85.1 : 14.9	$Pt_{5.67}Ni$	$Pt_{1.25}Ni$
Pt_2Ni/C	0.2704	57 : 43	18.9 : 1.5±0.41	76.3 : 23.7	$Pt_{3.22}Ni$	$Pt_{0.87}Ni$
Pt_3Ni/C	0.2724	49 : 51	19.3 : 1.8±0.07	79.1 : 20.9	$Pt_{3.79}Ni$	$Pt_{1.8}Ni$
Pt_5Ni/C	0.2749	43 : 57	14.8 : 0.82±0.08	85.6 : 14.4	$Pt_{5.95}Ni$	$Pt_{1.4}Ni$

*Determined by ICP-OES; †Nominal composition (20 wt.%);
[a]For Pt:Ni the ICP data is not reliable due to the low amount of sample;
‡Determined by XPS.

3.2. Surface Electrochemistry

The applied cyclic voltammetry technique in acid and alkaline media reveals the characteristic features of Pt, Figure 2. It is worth mentioning that, within the same experimental condition and error, the surface of all electrocatalysts did not show substantial modifications with respect to the measurements published [1] in the same $HClO_4$ acid medium, testifying the stability of the nanomaterials with time, as assessed by the XRD measurements (not shown here).

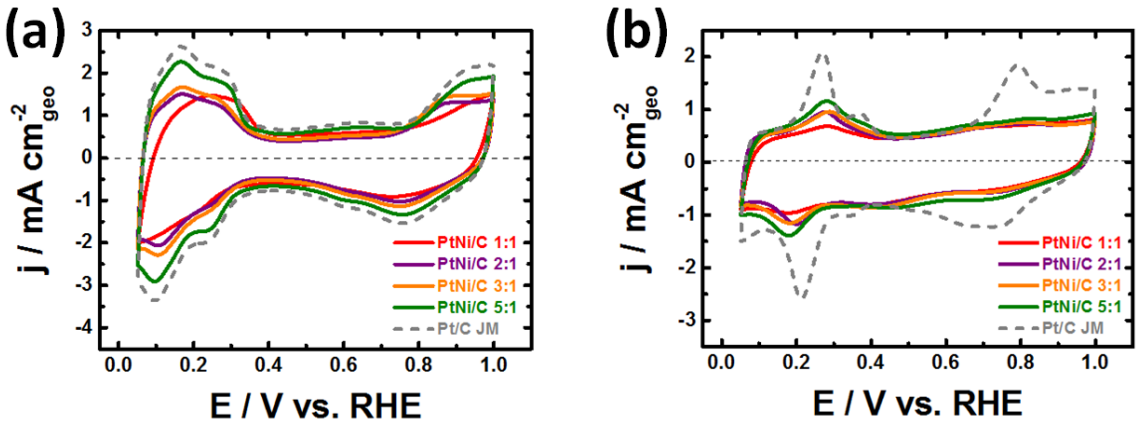

Figure 2. Cyclic voltammograms of Pt_xNi/C catalysts, as well as benchmark Pt/C JM catalyst: (a) N_2-saturated 0.1M $HClO_4$; and (b) N_2-saturated 0.1M KOH. Measurements were carried out at 50 mV s^{-1} and 25 °C.

As expected, the hydrogen underpotential region, H_{upd}, decreased by the presence of Ni atoms at the nanoparticles' surface in acid, and in alkaline medium, this phenomenon is testified by the OH-adsorption peak. The Pt-O reduction peak is strongly attenuated in alkaline medium. It is, furthermore, clear that the oxophilic power of Ni at the Pt:Ni NPs surfaces has a strong influence in alkaline medium, due to the high affinity of Ni to water, Ni centers provide OH_{ad} species to Pt neighboring centers. Then, due to the lack of OH in acid medium, the intensity of the Pt-O reduction peak is barely modified.

The oxidation of an adsorbed monolayer of carbon monoxide (CO-stripping) represents an electronic molecular probe that provides additional information of the Pt-CO bond strength [22] (see Figure 3). The CO oxidation on Pt/C JM, in acid medium, shows that the main CO-oxidation peak is centered at 0.81 V/RHE. The presence of Ni atoms at the nanoalloyed surface modifies the shape of the CO oxidation peak. For example, on Pt_5Ni/C catalyst, the main oxidation peak is centered at the same potential to that of Pt/C JM; on the other hand on Pt_3Ni/C, the main oxidation-peak is negatively shifted by 30 mV, and centered at 0.78 V/RHE, with a low-intensity pre-wave centered at ca. 0.73 V/RHE. For Pt_2Ni/C catalyst, we observe two different oxidation-peaks, one centered at ca. 0.81 V/RHE, and another one at 0.73 V/RHE; finally, on PtNi/C the oxidation peak is attained at 0.78 V/RHE. The presence of well-dispersed nanoparticles onto carbon support discards the particle-size effect phenomenon in the CO-oxidation multi-peak profile, as already reported by Yang et al. [1]. The amount of electron back-donation between the Pt *d*-orbital and the $2\pi^*$ antibonding orbital of CO is inversely proportional to CO desorption energy [23, 24]. The peak centered at ca. 0.73 V/RHE can be associated to the oxidation of carbon monoxide on Pt interacting with Ni atoms as suggested by Godinez et al. [25]. Therefore, the observed displacement of the main oxidation peak suggests a modification of the electronic structure of Pt, whose origin could be due to the strain effects in the nanoalloy. An analysis of the integrated charge of the systems shown in Figures 3(a) and (b) revealed that for Pt:Ni the ratio of the total charge of the CO-stripping in acid to alkaline is about 1.22, while on Pt/C JM is 1.17.

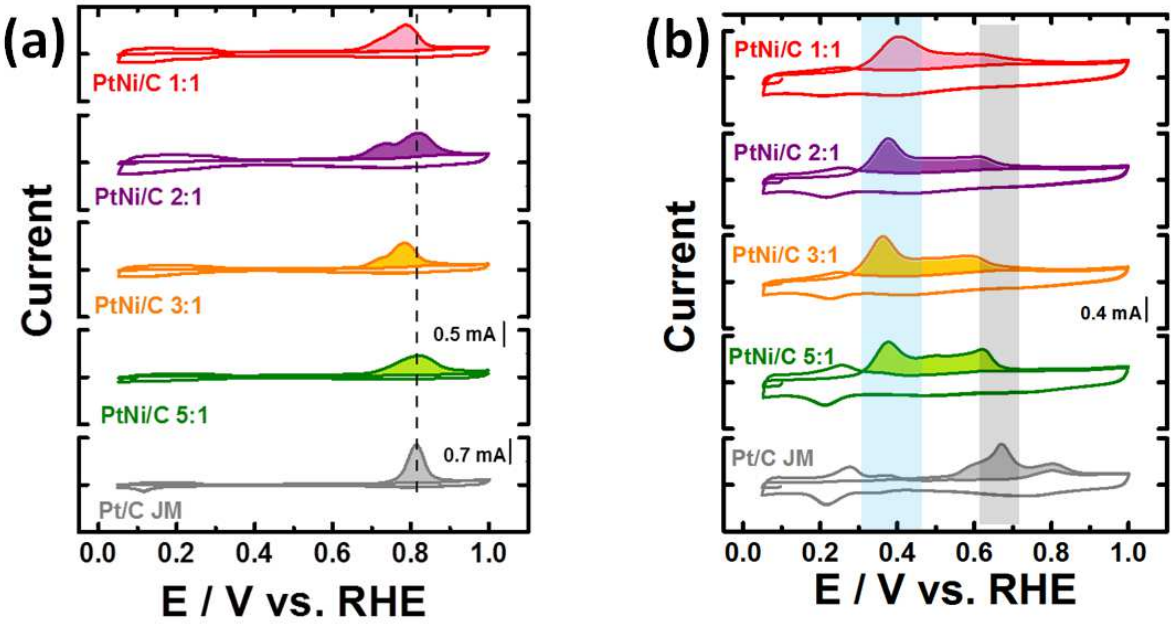

Figure 3. CO-stripping of Pt_xNi/C catalysts, and benchmark Pt/C JM catalyst in (a) 0.1M $HClO_4$; and (b) in 0.1M KOH. Measurements were carried out at 20 mV s^{-1} and 25 °C.

It is also of interest to mention that, at ca. 0.75 V, Figure 3(a), the adsorbed CO is oxidized in sites where Pt directly interacts with Ni. This signal has been observed on PtNi (111) (Pt-skin type) [26] and on unsupported PtNi nanosheets surfaces [27], supported by DFT-studies [26]. As expected, this feature is not present on the Pt/C JM material, further suggesting that it is attributed to the presence of Ni. The main CO oxidation process on the Pt sites is centered at ca. 0.8 V.

From the point of view of the interfacial charge in both acid and alkaline electrolytes, we can consider a similar behavior, as far as its magnitude is concerned, but not in the energetic extension in which this charge is distributed in the oxidation of CO in an alkaline medium. In alkaline electrolyte, unlike the acidic conditions, the presence of Ni modulates the CO-oxidation waves' shape. Figure 3(b) shows the presence of two main features, which are the pre-waves related to the early surface adsorption of OH (0.3 to 0.5 V/RHE) and the main CO-oxidation peak (at ca. 0.60 to 0.64 V/RHE). Therefore, the CO-oxidation process can be associated to a bifunctional mechanism, a consequence of the well-known oxophilicity of Ni (surface supply of OH^- species) according to equation (1):

$$CO_{ads} + OH_{ads} + OH^- \rightarrow CO_2 + e^- + H_2O \qquad (1)$$

3.3. Hydrogen Electrode Reaction in Alkaline Medium

In Figure 4, the HER/HOR polarization curves show that the electrochemical kinetics is also affected by the Ni content. An enhanced performance on Pt_5Ni/C and Pt_3Ni/C, with respect to Pt/C JM, is obtained, whereas the HER/HOR kinetics on Pt_2Ni/C and PtNi/C seems low. This observation suggests that the electrocatalyst must have an optimal Pt:Ni ratio to enhance the HER/HOR kinetics in alkaline medium.

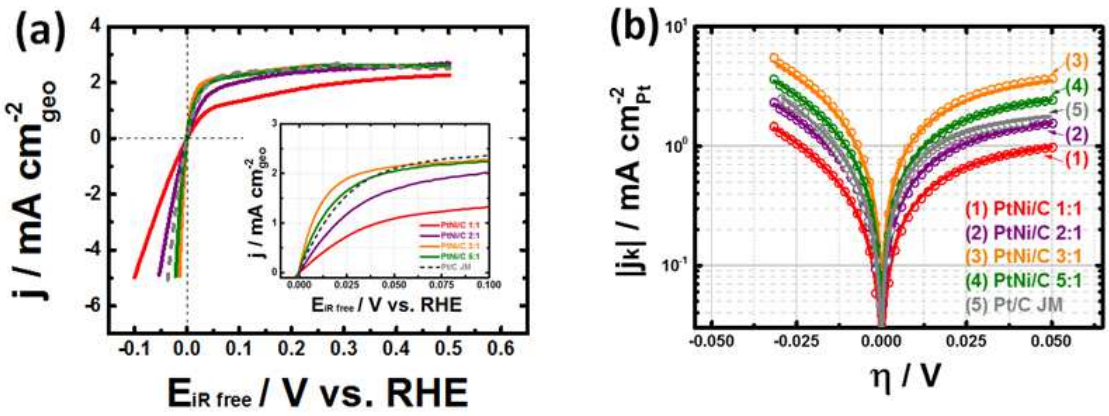

Figure 4. (a) iR-corrected HER/HOR polarization curves (Inset - HOR-branch). (b) extracted kinetic currents as function of overpotential of Pt_xNi/C, as well as Pt/C JM catalysts. Measurements were carried out in H_2-saturated 0.1M KOH, 5 mV s^{-1}, 1600 rpm, 25 °C.

From Tafel plots, Figure 4(b), the exchange current density, j_0, see data in Table 4, was extracted from the Butler-Volmer fitting and normalized by the Pt surface, calculated from the CO-stripping in acid medium. Due to the considerations discussed in section 3.2, about CO stripping in both acid and alkaline electrolytes, we considered, for the calculation of the real surface area, the integrated charge obtained in acid medium.

In addition, the branch corresponding to the HER polarization curves is shown in Figure 5. Herein, the well-known alkaline hydrogen-evolution wave on platinum (Pt/C JM) is contrasted. Again, differences in the activity on Pt_xNi/C, are observed.

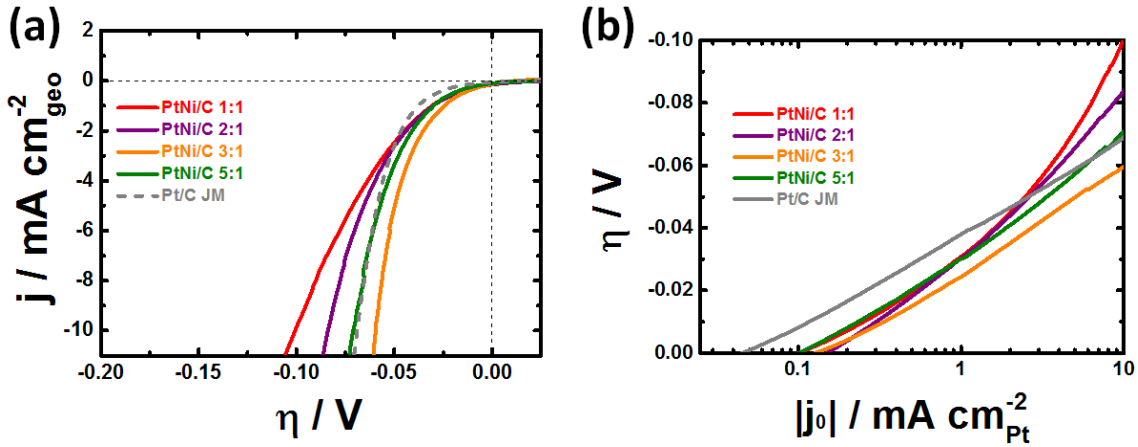

Figure 5. (a) iR-corrected HER polarization curves; and (b) the corresponding Tafel plots of Pt_xNi/C and Pt/C JM catalysts. Measurements were carried out in N_2-saturated 0.1M KOH, 5 mV s^{-1}, 1600 rpm, 25 °C.

At lower cathodic overpotential (0 to -0.05 V), the Pt_xNi/C catalysts outperform the Pt/C JM; meanwhile, at cathodic overpotential, < -0.05 V, the catalyst that outperforms Pt/C JM is Pt_3Ni/C. The observed kinetic enhancement for the HER/HOR in alkaline medium can be linked to the oxophilic power of Ni, since the energy barriers of water dissociation process, in alkaline medium, is weakened on Pt-coordinated to oxophilic species [10, 13, 28], e.g., Ni, whose oxygen-species (-OOH and -OH) can accelerate the Volmer step rate. This latter is considered as the reaction determining step (rds) in alkaline medium [12], equation (2).

$$H_2O + e^- \leftrightarrows H_{ads} + OH^- \qquad (2)$$

This statement is guaranteed by the results shown in figure 3(b). In other words, the Ni environment in the nanoalloy supply the reactive OH species to remove the H_{ads} intermediate via a bifunctional mechanism.

3.4. Oxygen Reduction Reaction in Alkaline Medium

The ORR polarization curves in alkaline medium of Pt_xNi/C and Pt/C JM catalysts are compared in Figure 6. The Ni atoms, again, modify the shape of the polarization curves. Various features can be observed, namely: (i) the ORR kinetic region (1.0 - 0.9 V/RHE) depends on the Pt to Ni ratio, and (ii) the magnitude of the limiting current density is also affected by the Ni atoms at the nanoalloy surfaces.

It is believed that, on PtNi catalysts, the electrons in Ni can be transferred to the *d*-orbital of Pt, promoting the filling of Pt *d*-band [29]. As a result, the *d*-band center of Pt is downshifted [29, 30]. This phenomenon has been observed on Pt:Ni based catalysts through the Pt 4f binding energy modifications [31, 32], and CO-stripping downshifted peaks [25, 31]. The enhancement of the ORR kinetics can be due to the fact that the bond strength between Pt and oxygen-species (-OOH and -OH) of the reaction intermediates are weakened.

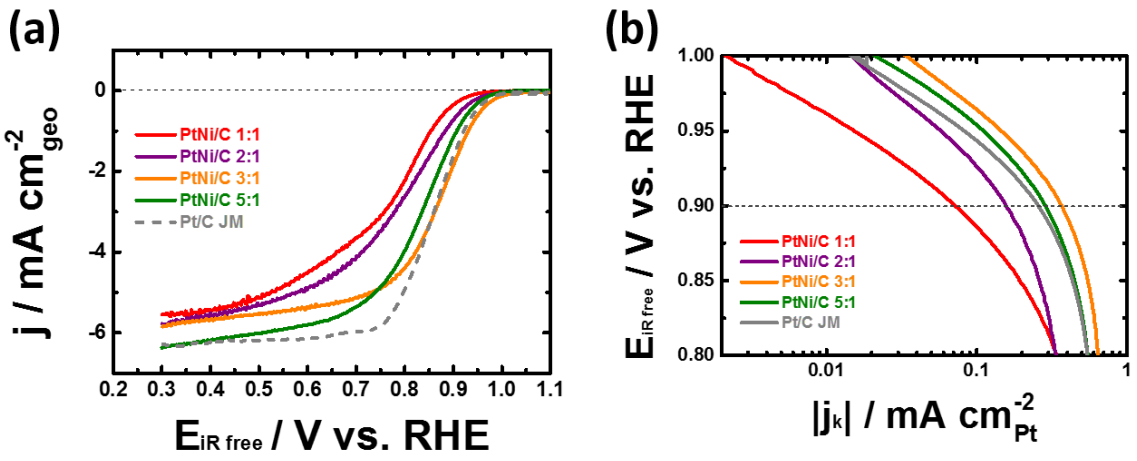

Figure 6. (a) iR-corrected ORR polarization curves; and (b) extracted kinetic currents as function of overpotential of Pt_xNi/C and Pt/C JM catalysts. Measurements were carried out in O_2-saturated 0.1M KOH, 5 mV s^{-1}, 1600 rpm, 25 °C.

Again, the oxophilic capacity of Ni promotes the formation of Ni oxides and/or hydroxide in the alkaline environment [29], favoring the transfer of electrons to oxygen because of the high electronegativity of this latter with respect to Pt (3.44 and 2.28, respectively) [29]. The oxidation of Ni promotes a loss of the number of transferred electrons between Pt and Ni at the surface. Since OH^- species are considered as spectators for the ORR [33], the presence of Ni oxides and/or hydroxide at the surface favors the screening effect on neighboring Pt atoms, inhibiting the diffusion of reactants across the surface, and the consequence is a decrease in the number of active sites for the ORR [30]. Paulus et al., [34] obtained similar kinetic parameters for pure Pt and Pt-alloys electrodes, suggesting that the reaction determining step, and the ORR mechanism, are identical on both. Therefore, the chemical rate constants and potential-dependent exponential terms in the Butler-Volmer equation are essentially the same, and the differences in the ORR kinetics relay on the coverage-dependent pre-exponential term, which in turn depends on the OH_{ads} coverage [34]. This discussion underpins the fact that the oxophilic effect, in alkaline medium, hinders the ORR electrochemical kinetics. The surface specific kinetic current density, j_s, extracted from Figure 6b, is reported in Table 4.

Table 4. Pt-Pt interatomic distance, exchange current density (HER/HOR), and surface specific kinetic current density (ORR) of Pt_xNi/C and Pt/C JM catalysts.

Catalysts	Pt-Pt distance (nm) [1]	j_0 (mA cm^{-2}_{Pt})	j_s@0.9V (mA cm^{-2}_{Pt})
Pt/C JM	0.2774	0.523±0.056	0.255±0.016
PtNi/C	0.2689	0.264±0.082	0.074±0.026
Pt_2Ni/C	0.2704	0.497±0.073	0.156±0.023
Pt_3Ni/C	0.2724	0.978±0.074	0.352±0.027
Pt_5Ni/C	0.2749	0.786±0.072	0.286±0.022

3.6 HER/HOR and ORR hierarchy of kinetic data on Pt:Ni nanoalloys

In order to correlate the different activities of the materials with the reactions of HER/HOR, ORR in alkaline electrolyte we thought that the Pt-Pt interatomic distance, Table 4, is a parameter that would account for the electronic state of the material, coupled with the chemical effect of nickel atoms. The exchange current density, j_0, for HER/HOR and the surface specific kinetic current density, j_s, at 0.9 V/RHE for ORR are plotted as a function of the interatomic Pt-Pt distance in Figure 7, from data in Table 4. We observe for j_0 and j_s a volcano-like shape, with a maximum in the electrocatalytic activity on the Pt_3Ni_1 nanoalloy.

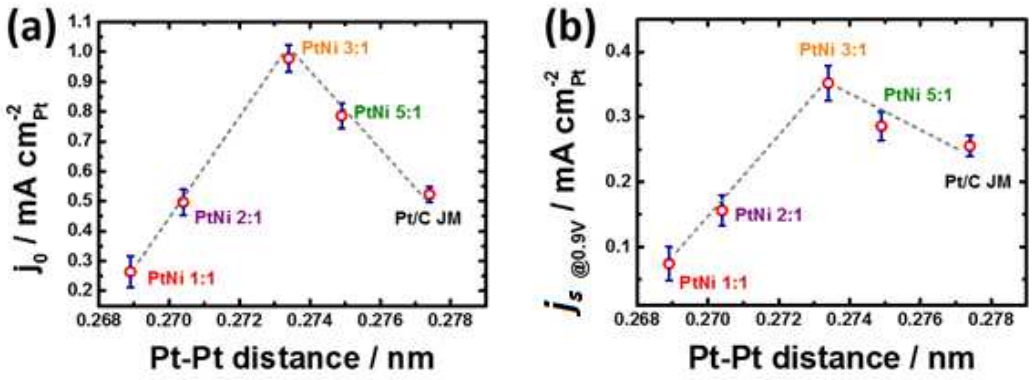

Figure 7. Volcano-like plot of our experimental data: (a) exchange current density (HER/HOR), (b) specific surface activity (ORR) of Pt_xNi/C catalysts and Pt/C JM materials, as function of the Pt-Pt interatomic distance.

Thus, an "optimal" Pt-Pt interatomic distance of 0.2734 nm enhances the above mentioned electrocatalytic process. We stress again that the oxophilic effect, seems to be crucial to accelerate the step considered as the *rds*: the Volmer step.

4. CONCLUSION

The HER/HOR and the ORR, in alkaline medium, are governed and enhanced by the materials' surface chemistry. Our results confirm that, for ORR, the so-called oxophilic effect hinders the electrochemical kinetics, since OH species promote the blocking of active surface sites. However, for the HER/HOR, the OH^- species act as reactive species, increasing the Volmer step rate. Nonetheless, the strain effect, induced the alloying of Pt with Ni, enhances the HER/HOR and ORR, wherein the Pt_3Ni composition seems to be the optimal stoichiometry, corresponding to a Pt-Pt interatomic distance of 0.2734 nm.

5. ACKNOWLEDGEMENTS

C.A.C.-R. acknowledges financial support from CONACYT-Mexico Nr.: MX-561206. The authors acknowledge financial support from the European Union (ERDF) and "Région Nouvelle Aquitaine".

6. REFERENCES

[1] H. Yang, W. Vogel, C. Lamy, N. Alonso-Vante, Structure and Electrocatalytic Activity of Carbon-Supported Pt-Ni Alloy Nanoparticles Toward the Oxygen Reduction Reaction, J. Phys. Chem. B, 108 (2004) 11024-11034.

[2] G. Merle, M. Wessling, K. Nijmeijer, Anion exchange membranes for alkaline fuel cells: A review, J. Membr. Sci., 377 (2011) 1-35.

[3] V. Vij, S. Sultan, A.M. Harzandi, A. Meena, J.N. Tiwari, W.-G. Lee, T. Yoon, K.S. Kim, Nickel-Based Electrocatalysts for Energy-Related Applications: Oxygen Reduction, Oxygen Evolution, and Hydrogen Evolution Reactions, ACS Catalysis, 7 (2017) 7196-7225.

[4] H. Osgood, S.V. Devaguptapu, H. Xu, J. Cho, G. Wu, Transition metal (Fe, Co, Ni, and Mn) oxides for oxygen reduction and evolution bifunctional catalysts in alkaline media, Nano Today, 11 (2016) 601-625.

[5] S. Zhao, L. Yan, H. Luo, W. Mustain, H. Xu, Recent progress and perspectives of bifunctional oxygen reduction/evolution catalyst development for regenerative anion exchange membrane fuel cells, Nano Energy, 47 (2018) 172-198.

[6] J. Durst, A. Siebel, C. Simon, F. Hasché, J. Herranz, H.A. Gasteiger, New insights into the electrochemical hydrogen oxidation and evolution reaction mechanism, Energy Environ. Sci., 7 (2014) 2255-2260.

[7] S. Lu, Z. Zhuang, Investigating the Influences of the Adsorbed Species on Catalytic Activity for Hydrogen Oxidation Reaction in Alkaline Electrolyte, Journal of the American Chemical Society 139 (2017) 5156–5163.

[8] Y. Jiang, X. Wu, Y. Yan, S. Luo, X. Li, J. Huang, H. Zhang, D. Yang, Coupling PtNi Ultrathin Nanowires with MXenes for Boosting Electrocatalytic Hydrogen Evolution in Both Acidic and Alkaline Solutions, Small, 15 (2019) e1805474.

[9] S.A. Abbas, S.H. Kim, M.I. Iqbal, S. Muhammad, W.S. Yoon, K.D. Jung, Synergistic effect of nano-Pt and Ni spine for HER in alkaline solution: hydrogen spillover from nano-Pt to Ni spine, Sci Rep, 8 (2018) 2986.

[10] Z. Cao, Q. Chen, J. Zhang, H. Li, Y. Jiang, S. Shen, G. Fu, B.A. Lu, Z. Xie, L. Zheng, Platinum-nickel alloy excavated nano-multipods with hexagonal close-packed structure and superior activity towards hydrogen evolution reaction, Nat Commun, 8 (2017) 15131.

[11] Z. Zhao, H. Liu, W. Gao, W. Xue, Z. Liu, J. Huang, X. Pan, Y. Huang, Surface-Engineered PtNi-O Nanostructure with Record-High Performance for Electrocatalytic Hydrogen Evolution Reaction, J Am Chem Soc, 140 (2018) 9046-9050.

[12] X. Yu, J. Zhao, L.-R. Zheng, Y. Tong, M. Zhang, G. Xu, C. Li, J. Ma, G. Shi, Hydrogen Evolution Reaction in Alkaline Media: Alpha- or Beta-Nickel Hydroxide on the Surface of Platinum?, ACS Energy Letters, 3 (2018) 237-244.

[13] Y. Wang, H. Zhuo, X. Zhang, X. Dai, K. Yu, C. Luan, L. Yu, Y. Xiao, J. Li, M. Wang, F. Gao, Synergistic effect between undercoordinated platinum atoms and defective nickel hydroxide on enhanced hydrogen evolution reaction in alkaline solution, Nano Energy, 48 (2018) 590-599.

[14] R. Subbaraman, D. Tripkovic, D. Strmcnik, K.C. Chang, M. Uchimura, A.P. Paulikas, V. Stamenkovic, N.M. Markovic, Enhancing hydrogen evolution activity in water splitting by tailoring Li(+)-$Ni(OH)_2$-Pt interfaces, Science, 334 (2011) 1256-1260.

[15] C.A. Campos-Roldán, N. Alonso-Vante, The Hydrogen Oxidation Reaction in Alkaline Medium: An Overview, Electrochemical Energy Reviews, (2019).
[16] M. Escudero-Escribano, P. Malacrida, M.H. Hansen, U.G. Vej-Hansen, A. Velázquez-Palenzuela, V. Tripkovic, J. Schiøtz, J. Rossmeisl, I.E.L. Stephens, I. Chorkendorff, Tuning the activity of Pt alloy electrocatalysts by means of the lanthanide contraction, Science, 352 (2016) 73-76.
[17] C.A. Campos-Roldán, R.G. González-Huerta, N. Alonso-Vante, Experimental Protocol for HOR and ORR in Alkaline Electrochemical Measurements, J. Electrochem. Soc., 165 (2018) J3001-J3007.
[18] K.J.J. Mayrhofer, G.K.H. Wiberg, M. Arenz, Impact of Glass Corrosion on the Electrocatalysis on Pt Electrodes in Alkaline Electrolyte, Journal of The Electrochemical Society, 155 (2008) P1.
[19] P.J. Rheinlander, J. Herranz, J. Durst, H.A. Gasteiger, Kinetics of the Hydrogen Oxidation/Evolution Reaction on Polycrystalline Platinum in Alkaline Electrolyte Reaction Order with Respect to Hydrogen Pressure, Journal of the Electrochemical Society, 161 (2014) F1448-F1457.
[20] M.C. Biesinger, B.P. Payne, A.P. Grosvenor, L.W.M. Lau, A.R. Gerson, R.S.C. Smart, Resolving surface chemical states in XPS analysis of first row transition metals, oxides and hydroxides: Cr, Mn, Fe, Co and Ni, Applied Surface Science, 257 (2011) 2717-2730.
[21] H.L. Skriver, N.M. Rosengaard, Surface energy and work function of elemental metals, Phys. Rev. B, 46 (1992) 7157-7168.
[22] C.A. Campos-Roldan, G. Ramos-Sanchez, R.G. Gonzalez-Huerta, J.R. Vargas Garcia, P.B. Balbuena, N. Alonso-Vante, Influence of sp^3-sp^2 Carbon Nanodomains on Metal/Support Interaction, Catalyst Durability, and Catalytic Activity for the Oxygen Reduction Reaction, ACS Appl Mater Interfaces, 8 (2016) 23260-23269.
[23] C.A. Campos-Roldán, R.G. González-Huerta, N. Alonso-Vante, The oxophilic and electronic effects on anchored platinum nanoparticles on sp^2 carbon sites: The hydrogen evolution and oxidation reactions in alkaline medium, Electrochim. Acta, 283 (2018) 1829-1834.
[24] G. Blyholder, Molecular orbital view of chemisorbed carbon monoxide, J. Phys. Chem., 68 (1964) 2772-2778.
[25] F. Godinez-Salomon, R. Mendoza-Cruz, M.J. Arellano-Jimenez, M. Jose-Yacaman, C.P. Rhodes, Metallic Two-Dimensional Nanoframes: Unsupported Hierarchical Nickel-Platinum Alloy Nanoarchitectures with Enhanced Electrochemical Oxygen Reduction Activity and Stability, ACS Appl Mater Interfaces, 9 (2017) 18660-18674.
[26] D.F. van der Vliet, C. Wang, D. Li, A.P. Paulikas, J. Greeley, R.B. Rankin, D. Strmcnik, D. Tripkovic, N.M. Markovic, V.R. Stamenkovic, Unique Electrochemical Adsorption Properties of Pt-Skin Surfaces, Angewandte Chemie International Edition, 51 (2012) 3139-3142.
[27] F. Godínez-Salomón, R. Mendoza-Cruz, M.J. Arellano-Jimenez, M. Jose-Yacaman, C.P. Rhodes, Metallic Two-Dimensional Nanoframes: Unsupported Hierarchical Nickel–Platinum Alloy Nanoarchitectures with Enhanced Electrochemical Oxygen Reduction Activity and Stability, ACS Applied Materials & Interfaces, 9 (2017) 18660-18674.
[28] N. Danilovic, R. Subbaraman, D. Strmcnik, K.C. Chang, A.P. Paulikas, V.R. Stamenkovic, N.M. Markovic, Enhancing the alkaline hydrogen evolution reaction

activity through the bifunctionality of $Ni(OH)_2$/metal catalysts, Angew Chem Int Ed Engl, 51 (2012) 12495-12498.
[29] S. Wang, L. Xiong, J. Bi, X. Zhang, G. Yang, S. Yang, Structural and Electronic Stabilization of PtNi Concave Octahedral Nanoparticles by P Doping for Oxygen Reduction Reaction in Alkaline Electrolytes, ACS Appl Mater Interfaces, 10 (2018) 27009-27018.
[30] F.H.B. Lima, J.R.C. Salgado, E.R. Gonzalez, E.A. Ticianelli, Electrocatalytic Properties of PtCo⁄C and PtNi⁄C alloys for the Oxygen Reduction Reaction in Alkaline Solution, Journal of The Electrochemical Society, 154 (2007) A369.
[31] Y. Hao, X. Wang, Y. Zheng, J. Shen, J. Yuan, A.-j. Wang, L. Niu, S. Huang, Size-controllable synthesis of ultrafine PtNi nanoparticles uniformly deposited on reduced graphene oxide as advanced anode catalysts for methanol oxidation, International Journal of Hydrogen Energy, 41 (2016) 9303-9311.
[32] T.-W. Chen, J.-X. Kang, D.-F. Zhang, L. Guo, Ultralong PtNi alloy nanowires enabled by the coordination effect with superior ORR durability, RSC Advances, 6 (2016) 71501-71506.
[33] D. Strmcnik, M. Escudero-Escribano, K. Kodama, V.R. Stamenkovic, A. Cuesta, N.M. Markovic, Enhanced electrocatalysis of the oxygen reduction reaction based on patterning of platinum surfaces with cyanide, Nat Chem, 2 (2010) 880-885.
[34] U.A. Paulus, A. Wokaun, G.G. Scherer, T.J. Schmidt, V. Stamenkovic, N.M. Markovic, P.N. Ross, Oxygen reduction on high surface area Pt-based alloy catalysts in comparison to well defined smooth bulk alloy electrodes, Electrochimica Acta, 47 (2002) 3787-3798.